

RESEARCH MEMORANDUM

STATIC LATERAL STABILITY CHARACTERISTICS OF A $\frac{1}{10}$ -SCALE
MODEL OF THE X-1 AIRPLANE AT HIGH SUBSONIC MACH NUMBERS

By Richard E. Kuhn and James W. Wiggins

Langley Aeronautical Laboratory
Langley Field, Va.

NATIONAL ADVISORY COMMITTEE
FOR AERONAUTICS

WASHINGTON

August 8, 1951

NATIONAL ADVISORY COMMITTEE FOR AERONAUTICS

RESEARCH MEMORANDUM

STATIC LATERAL STABILITY CHARACTERISTICS OF A $\frac{1}{10}$ -SCALE

MODEL OF THE X-1 AIRPLANE AT HIGH SUBSONIC MACH NUMBERS

By Richard E. Kuhn and James W. Wiggins

SUMMARY

A wind-tunnel investigation was conducted to determine the static lateral stability characteristics of a $\frac{1}{10}$ -scale model of the X-1 transonic research airplane in the Mach number range from 0.40 to 0.88. The lateral stability parameters agree well with previously obtained low-speed data and exhibit the expected slight increase in magnitude with Mach number. The horizontal stabilizer had very little effect on the lateral stability parameters within the range of these tests.

INTRODUCTION

Results of flight tests of the X-1 transonic research airplane (reference 1) have shown unsatisfactory damping of lateral oscillations, particularly when the amplitude of these oscillations was of the order of one degree. Some analyses of the dynamic lateral behavior of the airplane have been made (reference 2, for example); however, for the most part, these analyses have been based on aerodynamic information from low-speed wind-tunnel tests (reference 3). Consequently, in order to provide some experimental information at high subsonic Mach numbers, an investigation of the high-speed lateral stability characteristics of a $\frac{1}{10}$ -scale model of the X-1 airplane was conducted in the Langley high-speed 7- by 10-foot tunnel.

Inasmuch as the flow in the region of the vertical tail was thought to be particularly critical, the investigation was undertaken with special consideration being given to minimizing the effects of the

support system on the flow in the region of the tail. The effect of the horizontal stabilizer on the effectiveness of the vertical tail was also investigated.

SYMBOLS AND COEFFICIENTS

The stability system of axes used for the presentation of the data, together with an indication of the positive forces, moments, and angles, is presented in figure 1. All moments presented here are referred to the center of gravity of the airplane.

C_L	lift coefficient (Lift/qS)
C_l	rolling-moment coefficient (Rolling moment/qSb)
C_n	yawing-moment coefficient (Yawing moment/qSb)
C_Y	lateral-force coefficient (Lateral force/qS)
q	dynamic pressure, pounds per square foot $\left(\rho V^2/2\right)$
ρ	mass density of air, slugs per cubic foot
V	free-stream velocity, feet per second
S	wing area, square feet
b	wing span, feet
c	wing chord
\bar{c}	mean aerodynamic chord, feet
ψ	angle of yaw, degrees
α	angle of attack of airplane reference axis, degrees
i_t	incidence of the horizontal stabilizer, degrees
M	Mach number (V/a)
a	velocity of sound, feet per second

R	Reynolds number ($\rho V \bar{c} / \mu$)
C	wing chord, feet
μ	absolute viscosity of air, slugs per foot-second

$$C_{l_{\psi}} = \frac{\partial C_l}{\partial \psi}$$

$$C_{n_{\psi}} = \frac{\partial C_n}{\partial \psi}$$

$$C_{Y_{\psi}} = \frac{\partial C_Y}{\partial \psi}$$

Subscripts

vt	vertical tail
f	fuselage
M	Mach number
w	wing

APPARATUS AND METHODS

Model

The wing and horizontal and vertical tails were constructed of an aluminum alloy, whereas the fuselage was of a composite construction consisting of a steel core with a bismuth tin covering to give the external contour. The dorsal and ventral fins were constructed of mahogany.

Details of the model as tested are presented in figure 2, and a cutaway view of the model showing the arrangement by which the wing, the electrical strain-gage balance, and the fuselage are incorporated is shown in figure 3.

Support System

In order to minimize the effect of the support system on the air flow in the region of the tail, a yoke-type support system was used

(fig. 4). The yoke stings extended rearward from the wing tips to a streamlined vertical strut located in the tunnel diffuser aft of the test section. Angles of yaw were obtained through the use of various couplings located in the two stings at the elbows of the yoke (fig. 4), and angles of attack were obtained by the use of various wing blocks.

Inasmuch as an internal electrical strain-gage balance was used for the tests, the wings of the model served as a part of the support system. The aft end of the balance was attached to the inner steel shell, which, in turn, was supported by the wing and yoke sting (fig. 3). The fuselage was attached to the unsupported forward end of the balance; thus all forces and moments measured on the balance are attributable only to the fuselage and tail in the presence of the wing.

In order to minimize leakage at the wing-fuselage juncture, a sponge seal was used as shown in figures 4 and 5. The seal was attached to the square cut base section of the wing and was free to slide on the internal surface of the fuselage. A static calibration of the balance with and without the sponge seal indicated that this seal had no measurable effect on the data.

The electrical leads from the strain-gage balance extended through the aft end of the fuselage into a small steel tube extending forward from the vertical strut (fig. 4).

TESTS

The model was tested in the Langley high-speed 7- by 10-foot tunnel through a Mach number range from 0.40 to 0.88 at angles of yaw of 0° , $\pm 1^\circ$, $\pm 2^\circ$, $\pm 3^\circ$, and $\pm 4^\circ$ and at angles of attack of 0° and 4° . The variation of test Reynolds number with Mach number is presented in figure 6.

CORRECTIONS

The type of support used minimizes any tare effects that are apt to be experienced by the fuselage and tail, and therefore no tare corrections have been applied to these data. The angles of attack and yaw have, however, been corrected for the deflection of the stings and strain-gage balance under load. The corrections due to the jet-boundary induced upwash were computed and found to be negligible and therefore have not been applied. Dynamic pressure and Mach number have been corrected for blocking by the model and its wake by the method of reference 4.

RESULTS AND DISCUSSION

The results of the investigation are presented in the following figures. The lift coefficients indicated on the figures were estimated from reference 5.

Figure

Fuselage and tail data (in presence of wing):

$\alpha = 0^\circ$		
Horizontal stabilizer incidence	$i_t = 2.5^\circ$	7
Horizontal stabilizer incidence	$i_t = 0.7^\circ$	8
Horizontal tail off		9
Fuselage alone (in presence of wing)		10
$\alpha = 4^\circ$		
Horizontal stabilizer incidence	$i_t = 2.5^\circ$	11
Horizontal stabilizer incidence	$i_t = 0.7^\circ$	12
Horizontal tail off		13
Fuselage alone (in presence of wing)		14
Lateral stability parameters:		
$\alpha = 0^\circ$		15
$\alpha = 4^\circ$		16
Comparison with estimated characteristics		17

The lateral stability parameters determined in this investigation (figs. 15 and 16) exhibit the expected slight increase in magnitude with Mach number in the test range and can be extrapolated to the low-speed values from reference 3. It should be emphasized that these data are for the fuselage and tail in the presence of the wing, whereas the values from reference 3 are for the complete model. While it might be expected that this difference of configuration would cause some discrepancy, an examination of the low-speed data (fig. 9 of reference 3) indicates that at angles of attack and yaw up to 4° there is very little effect of the wing on the lateral stability parameters; therefore, up to the force break at least, the fuselage-tail data represent the only important contribution to the lateral stability.

It is of interest to compare the measured contribution of the empennage to the directional and lateral stability throughout the Mach number range with the estimated contribution that would be calculated from the low-speed data (reference 3). For these calculations the wing-fuselage contribution was assumed to be unaffected by compressibility and only the tail contribution was corrected for Mach number effects. These

calculations have been made by calculating the lift-curve slope of the vertical tail by using the following relation

$$C_{L_{\alpha_{vt}}}_{M \rightarrow 0} = C_{Y_{\psi_{vt}}}_{M \rightarrow 0} \frac{S_w}{S_{vt}}$$

(where $C_{Y_{\psi_{vt}}}_{M \rightarrow 0}$ is the side-force contribution of the vertical tail

obtained from reference 3) and then determining the effective aspect ratio from the charts of reference 6. The variation of $C_{L_{\alpha_{vt}}}$ through the

Mach number range for this effective aspect ratio was determined by application of the Prandtl-Glauert transformation as suggested in reference 6. The side-force contribution of the vertical tail through the Mach number range was then obtained from the expression

$$C_{Y_{\psi_{vt}}}_{M} = C_{L_{\alpha_{vt}}}_{M} \frac{S_{vt}}{S_w}$$

The yawing-moment ($C_{n_{\psi_{vt}}}$) and rolling-moment ($C_{l_{\psi_{vt}}}$) parameters were calculated by assuming that the effective center of pressure of the vertical tail was unaffected by compressibility.

The excellent agreement between the measured values of this report and the calculated values (fig. 17) indicate the reliability of this calculation procedure for this airplane.

A study of figures 15 and 16 indicates very little effect of the horizontal tail on the lateral stability parameters except at the highest Mach numbers. This result is also in qualitative agreement with the data of reference 7 which indicate only a small change in effective aspect ratio of the vertical tail due to the presence of the horizontal tail at this particular location on the vertical tail.

The stabilizer angles used represent the extremes of tail loads necessary to balance the wing-fuselage pitching moment experienced in the range of these tests. The reason for the slight reduction in effective dihedral ($C_{l_{\psi}}$) at the highest Mach numbers due to the addition of the horizontal tail (fig. 15) is not completely understood; however, it may

be due to a negative dihedral contribution of the horizontal tail resulting from an asymmetrical load distribution at these Mach numbers.

The data at the higher Mach numbers (above $M = 0.83$) indicate some nonlinear results particularly in the yawing-moment and rolling-moment coefficients (figs. 7 to 13). The reasons for these nonlinear tendencies are not understood although there are several possible contributing factors. An examination of the data of reference 5 indicates a possible breakdown of the flow on the wing at a Mach number of about 0.83 which may affect the flow on the tail. It should also be pointed out that above a Mach number of 0.83 the entire support system was observed to shake rather violently. An investigation established the fact that the tunnel was not choked; however, it is believed that a strong shock existed at the intersection of the vertical strut and the arms of the yoke and this shock may have been intense enough to disturb the flow in the region of the tail. Because of these uncertainties the data at these Mach numbers have not been analyzed, even though they are presented. However, it is apparent from the data that no reduction in stability is exhibited. Tuft studies of the flow on the vertical tail and on the rear portion of the fuselage showed no indication of flow separation throughout the Mach number range.

CONCLUSIONS

Based on the high-speed wind-tunnel tests of the static lateral stability characteristics of a $\frac{1}{10}$ -scale model of the X-1 transonic research airplane in the Mach number range from 0.40 to 0.88, the following conclusions have been drawn:

1. The measured contribution of the tail to the directional and lateral stability agreed well with that calculated from low-speed data throughout the Mach number range investigated.
2. The horizontal stabilizer had very little effect on the lateral stability parameters within the range of these tests.

Langley Aeronautical Laboratory
National Advisory Committee for Aeronautics
Langley Field, Va.

REFERENCES

1. Williams, Walter C., Forsyth, Charles M., and Brown, Beverly P.: General Handling-Qualities Results Obtained during Acceptance Flight Tests of the Bell XS-1 Airplane. NACA RM L8A09, 1948.
2. Polhamus, Edward C.: A Study of the Dynamic Stability of the Bell X-1 Research Airplane. NACA RM L9K04a, 1950.
3. Kemp, W. B., and Polhamus, E. C.: Wind-Tunnel Tests of a $\frac{1}{4}$ -Scale Model of the Bell XS-1 Transonic Airplane (Army Project MX-653). II - Lateral and Directional Stability and Control. NACA MR L6E27, Army Air Forces and Bur. Aero, 1946.
4. Herriot, John G.: Blockage Corrections for Three-Dimensional-Flow Closed-Throat Wind Tunnels, with Consideration of the Effect of Compressibility. NACA Rep. 995, 1950. (Formerly NACA RM A7B28.)
5. Mattson, Axel T., and Loving, Donald L.: Force, Static Longitudinal Stability, and Control Characteristics of a $\frac{1}{16}$ -Scale Model of the Bell XS-1 Transonic Research Airplane at High Mach Numbers. NACA RM L8A12, 1948.
6. DeYoung, John: Theoretical Additional Span Loading Characteristics of Wings with Arbitrary Sweep, Aspect Ratio, and Taper Ratio. NACA TN 1491, 1947.
7. Murray, Harry E.: Wind-Tunnel Investigation of End-Plate Effects of Horizontal Tails on a Vertical Tail Compared with Available Theory. NACA TN 1050, 1946.

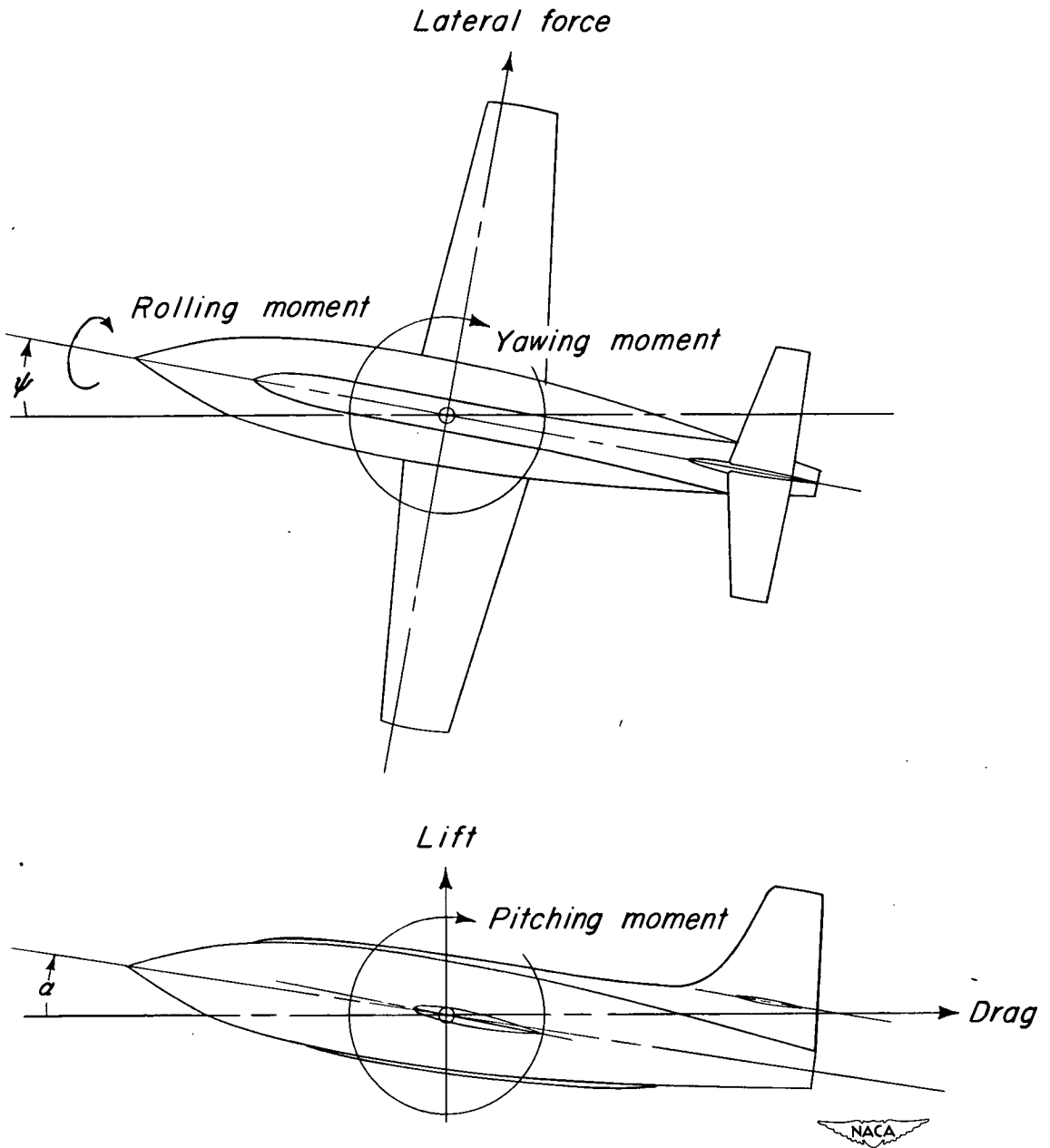


Figure 1.- System of axes. Positive values of forces, moments, and angles are indicated by arrows.

Areas Sq ft	
Wing	1.30
Horizontal tail	.260
Vertical tail	.344
Airfoil section	NACA 65,-110
Root and tip	
Wing incidence	
Root chord to fuselage	2.5°
Tip chord to fuselage	1.5°

Note: All dimensions in inches.

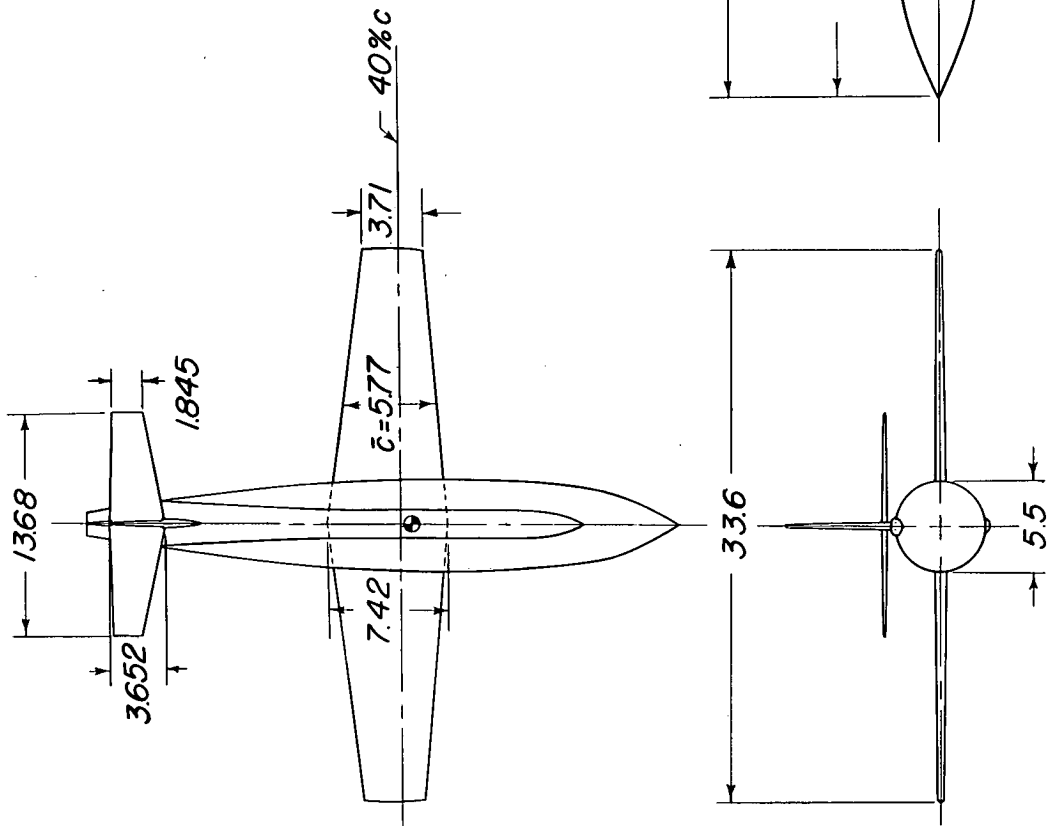


Figure 2.- Three-view drawing of the $\frac{1}{10}$ -scale model of the X-1 transonic research airplane.

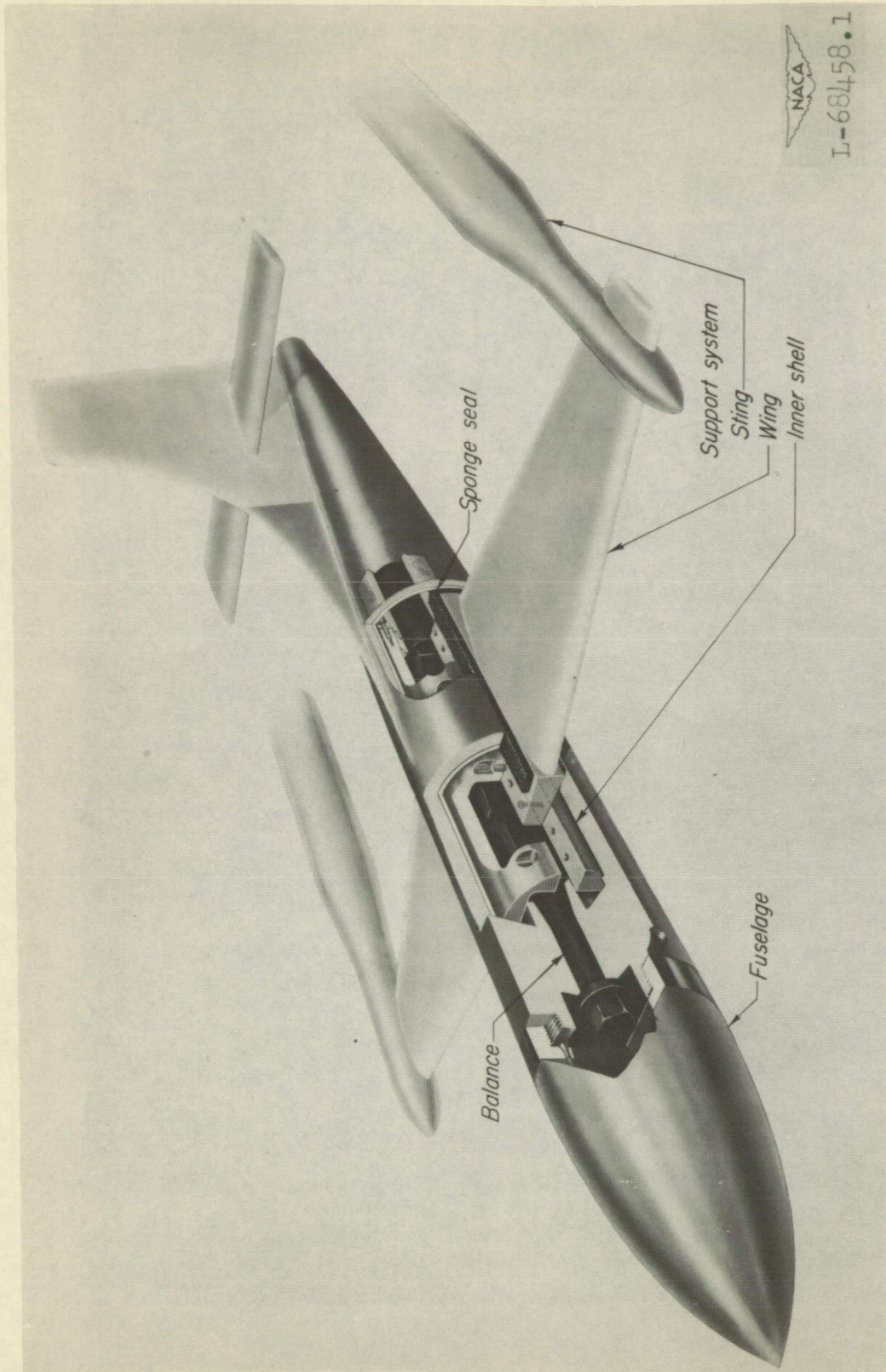


Figure 3.- Cutaway view of model.

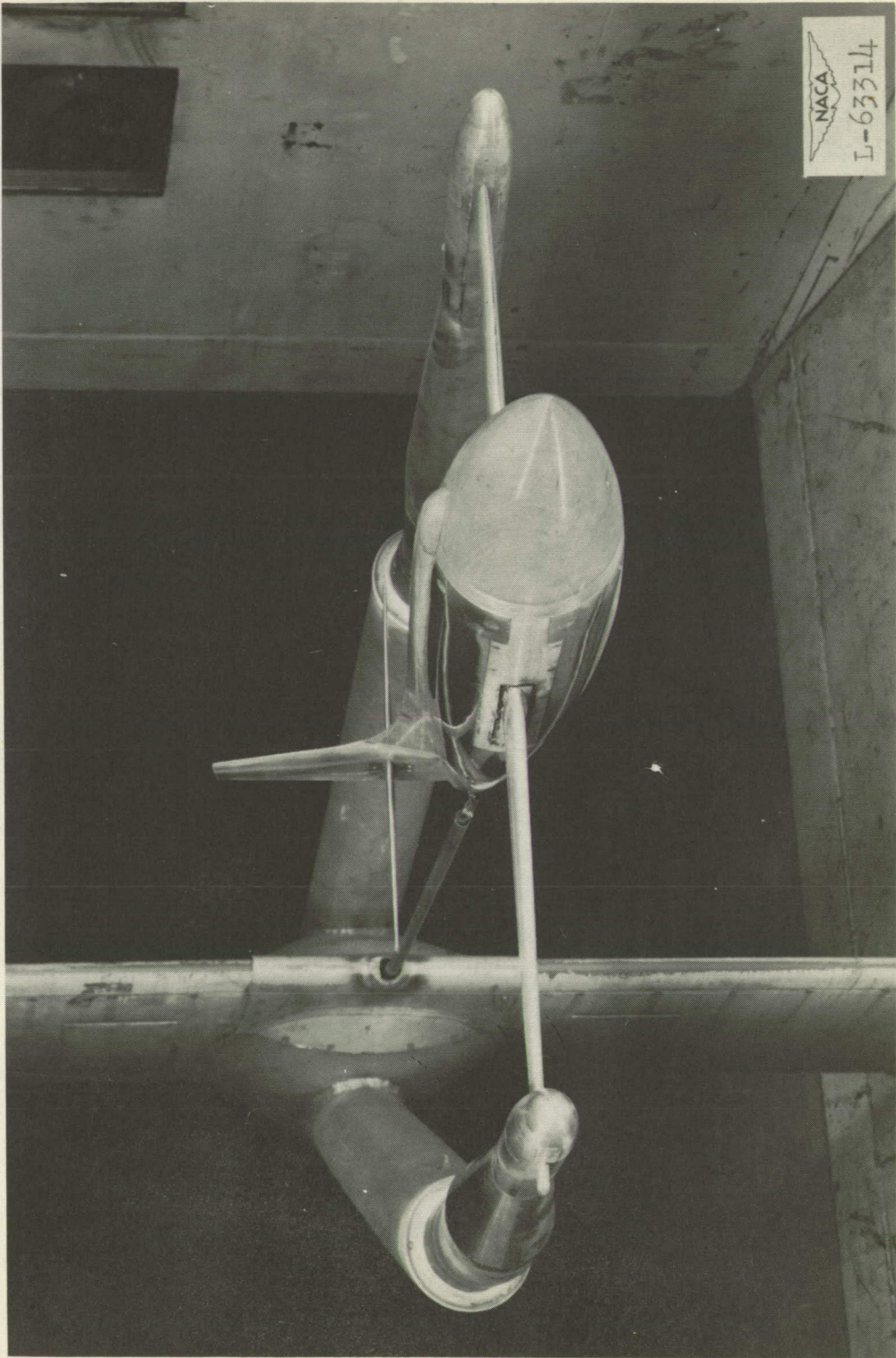


Figure 4.- Photograph of model and support system.



Figure 5.- Photograph of wing-fuselage juncture showing sponge seal.

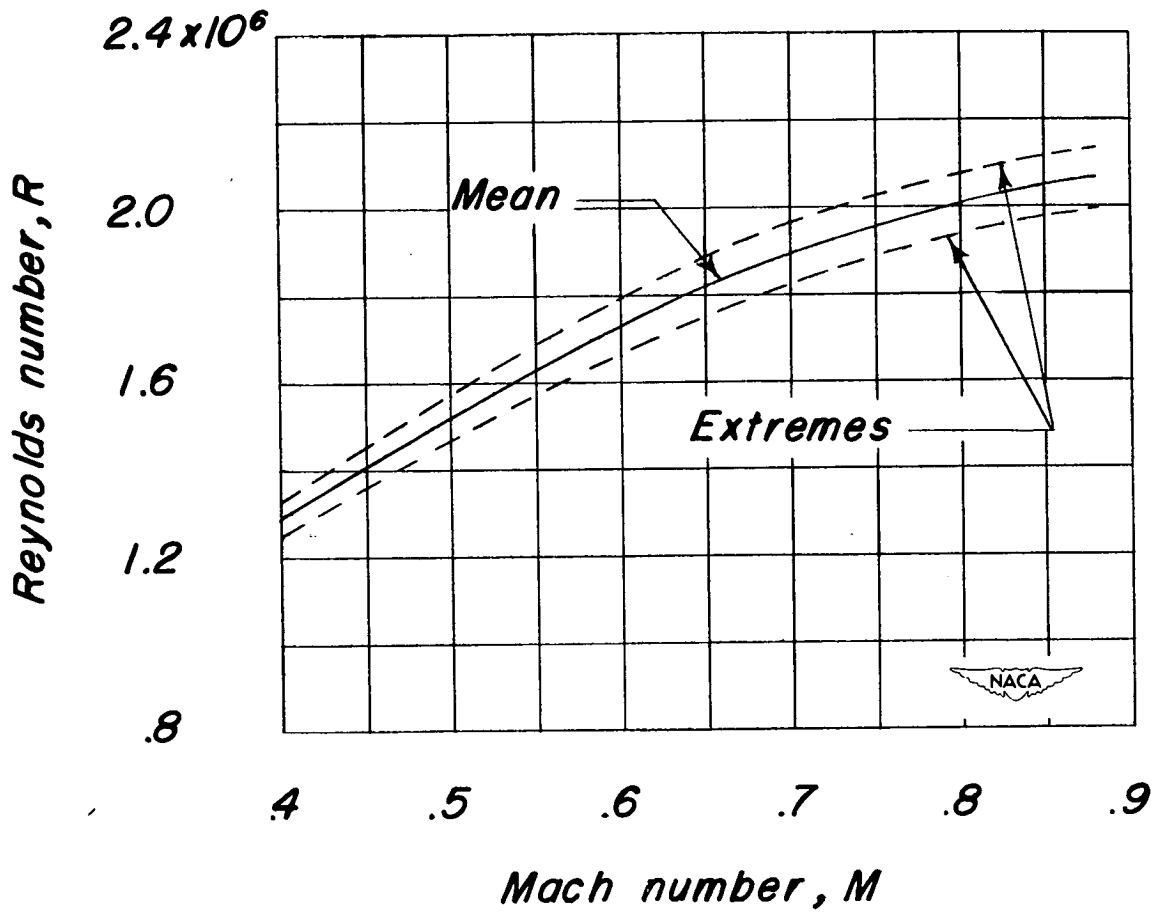


Figure 6.- Variation of test Reynolds number with Mach number.

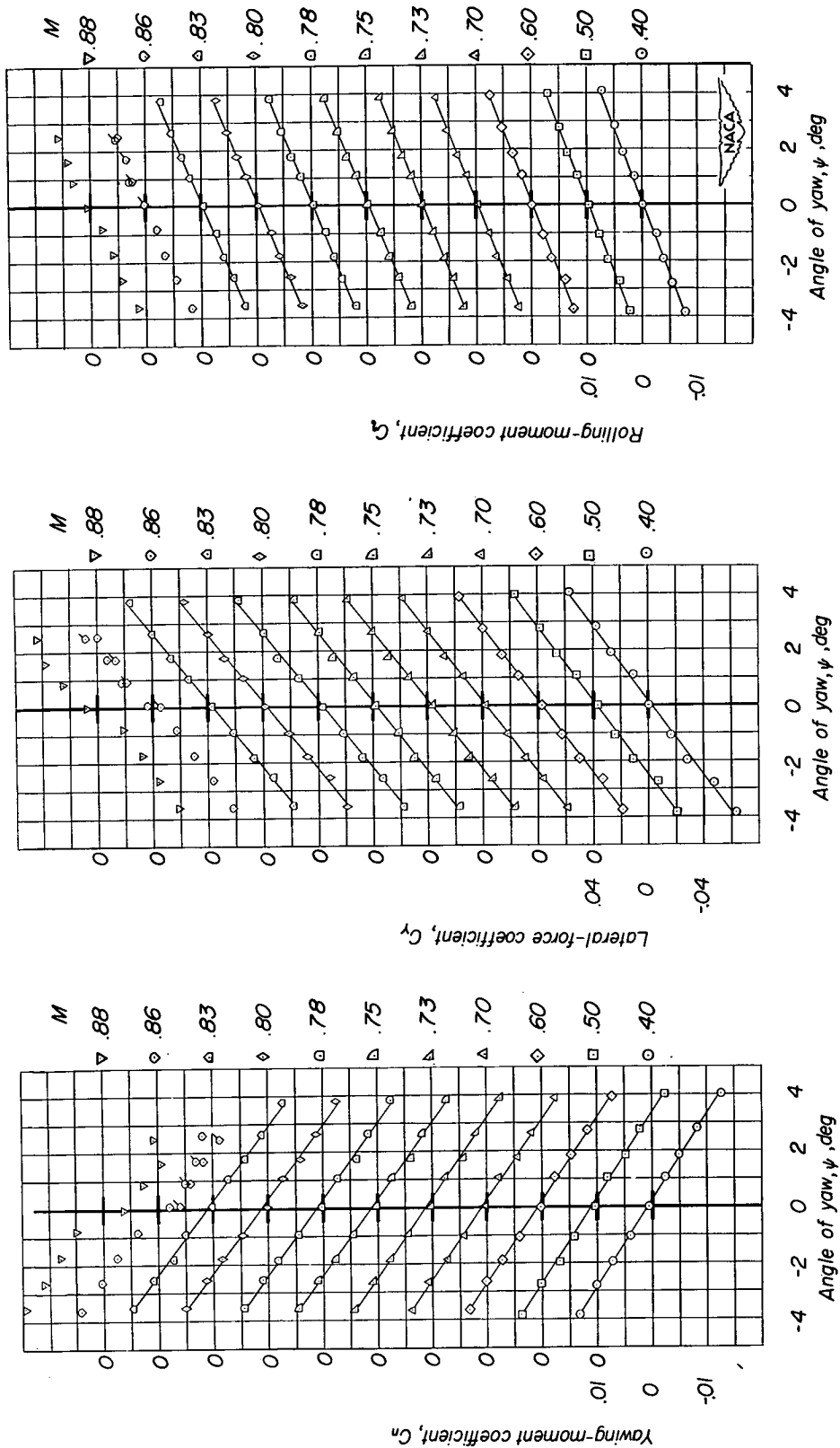


Figure 7.- Aerodynamic characteristics in yaw of the $\frac{1}{10}$ -scale model of the X-1 airplane. Fuselage-tail configuration in presence of wing. $i_t = 2.5^\circ$; $\alpha = 0^\circ$; $C_L \approx 0.30$.

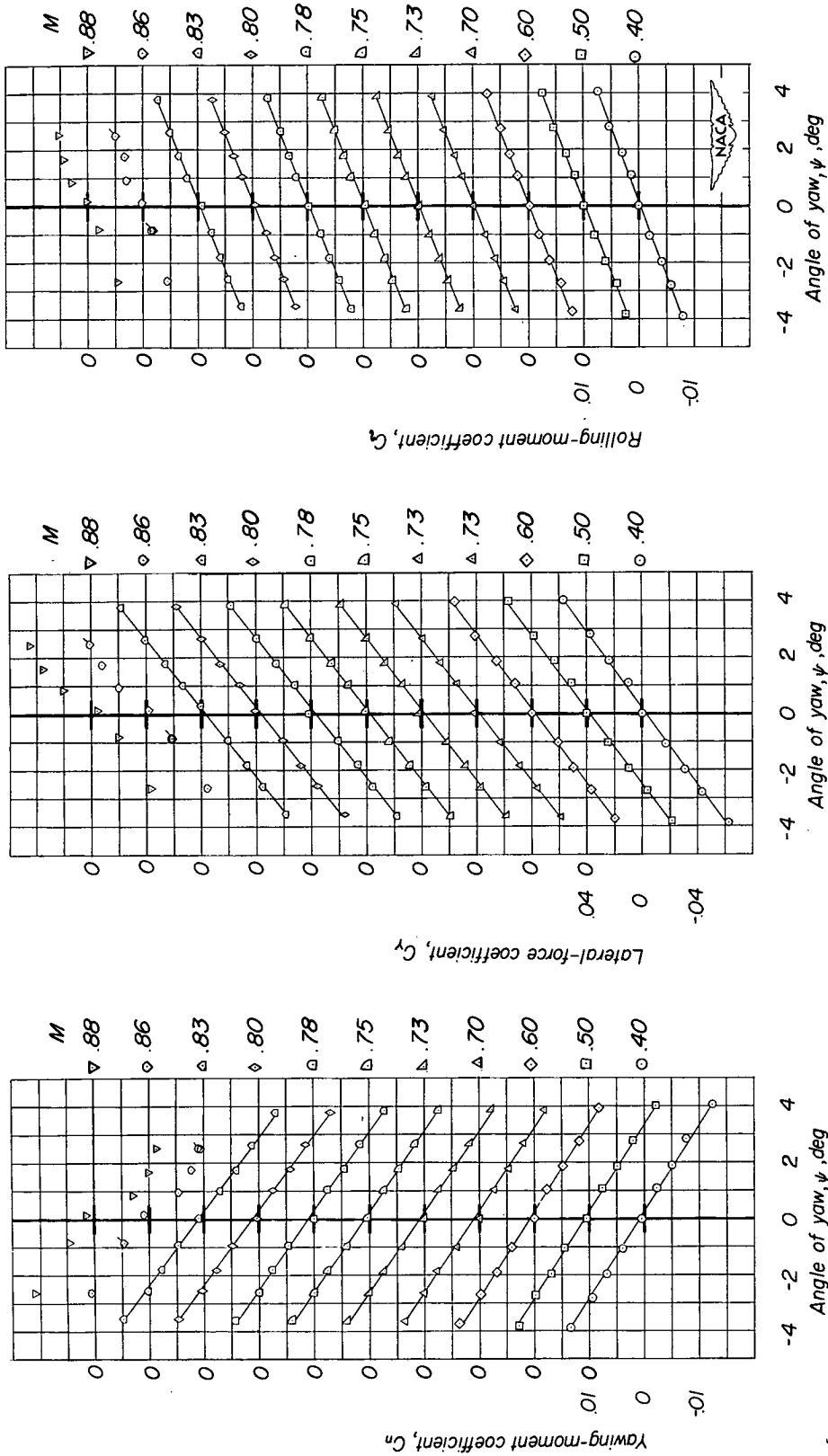


Figure 8.- Aerodynamic characteristics in yaw of the $\frac{1}{10}$ -scale model of the X-1 airplane. Fuselage-tail configuration in presence of wing. $i_t = 0.7^\circ$; $\alpha = 0^\circ$; $C_L \approx 0.25$.

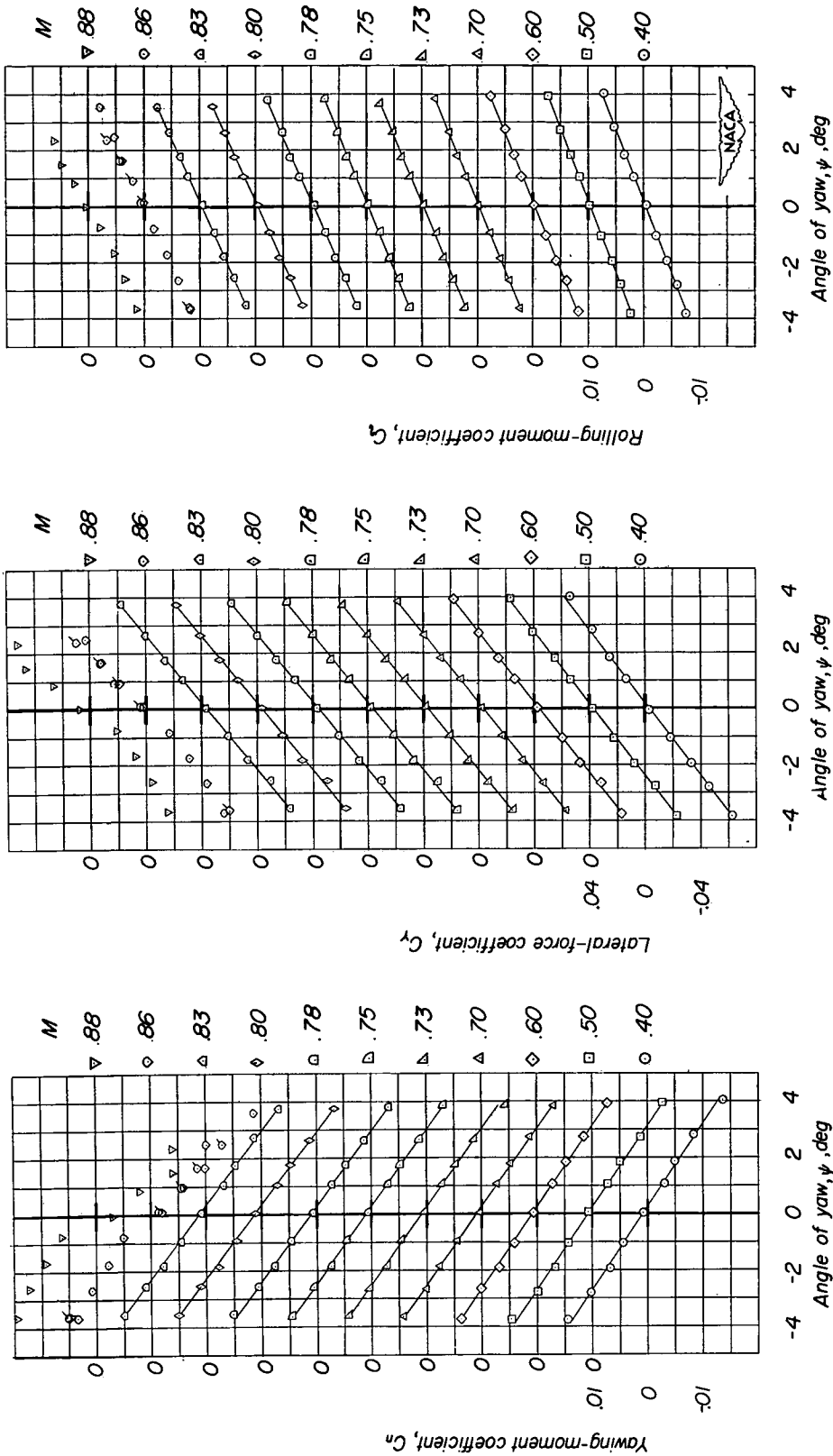


Figure 9.- Aerodynamic characteristics in yaw of the $\frac{1}{10}$ -scale model of the X-1 airplane. Horizontal tail off. $\alpha = 0^\circ$; $C_L \approx 0.25$.

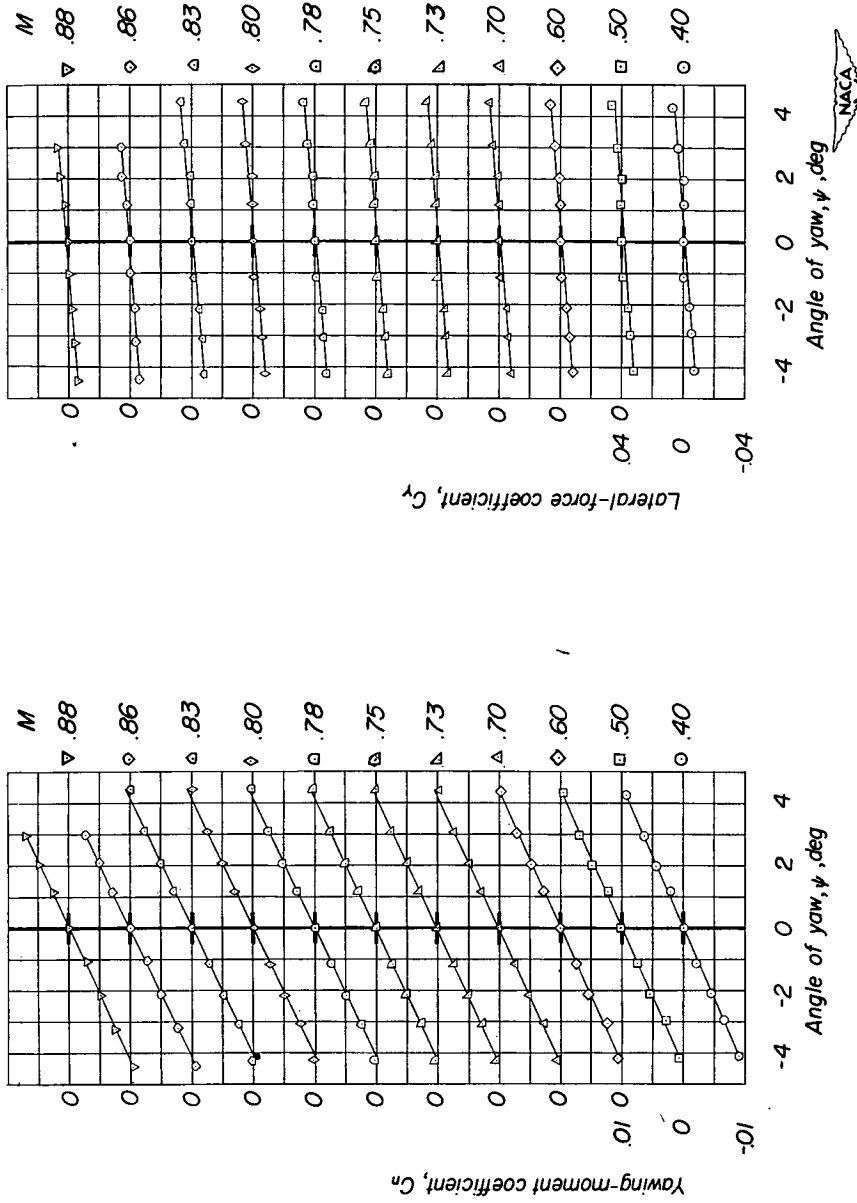


Figure 10.- Aerodynamic characteristics in yaw of the $\frac{1}{10}$ -scale model of the X-1 airplane. Horizontal and vertical tail off. $\alpha = 0^\circ$; $C_L \approx 0.25$.

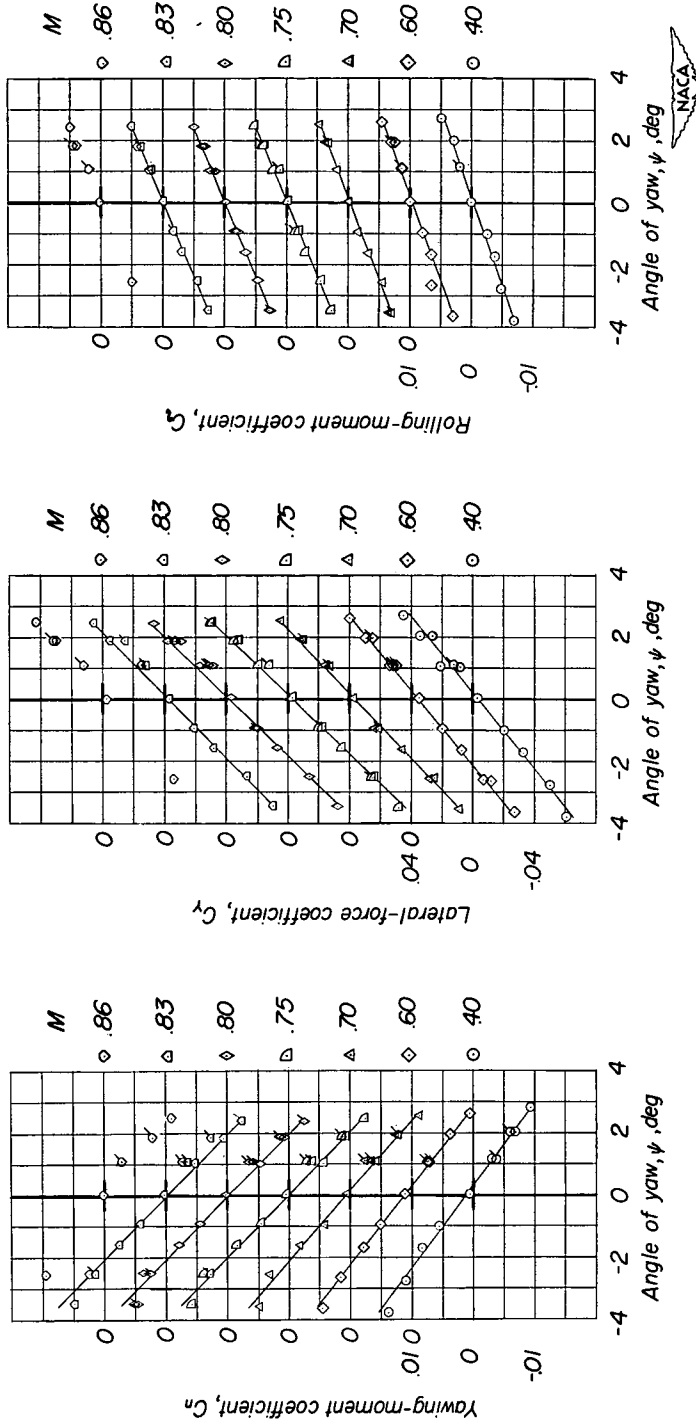


Figure 11.- Aerodynamic characteristics in yaw of the $\frac{1}{10}$ -scale model of the X-1 airplane. Fuselage-tail configuration in presence of wing. $i_t = 2.5^\circ$; $\alpha = 4^\circ$; $C_L \approx 0.65$.

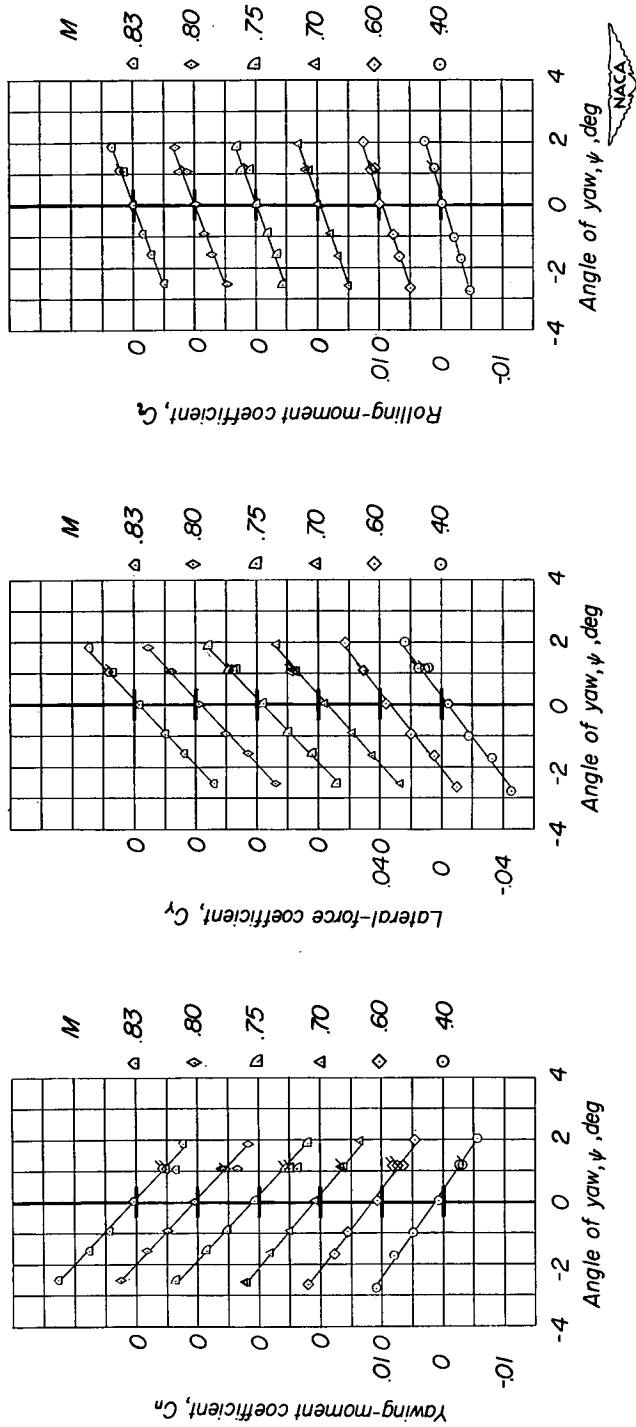


Figure 12.- Aerodynamic characteristics in yaw of the $\frac{1}{10}$ -scale model of the X-1 airplane. Fuselage-tail configuration in presence of wing. $i_t = 0.7^\circ$; $\alpha = 4^\circ$; $C_L \approx 0.60$.

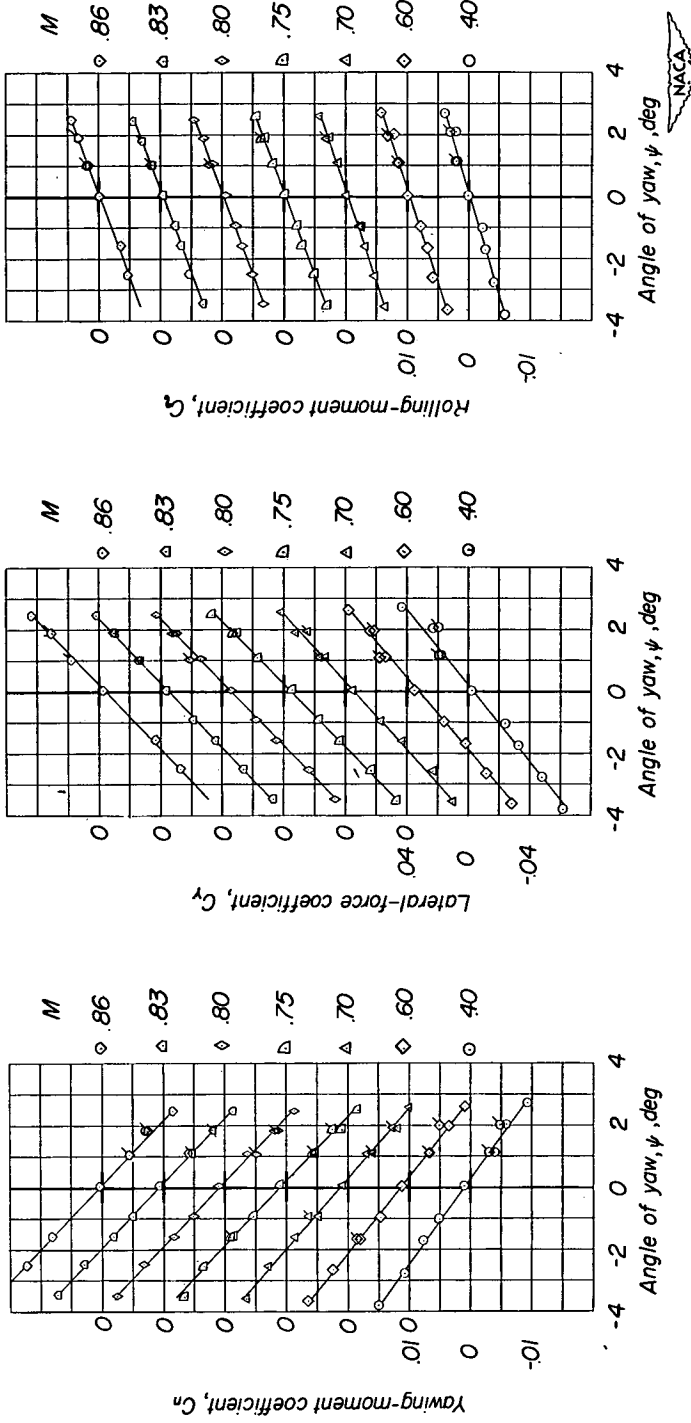


Figure 13.- Aerodynamic characteristics in yaw of the $\frac{1}{10}$ -scale model of the X-1 airplane. Horizontal tail off. $\alpha = 4^\circ$; $C_L \approx 0.60$.

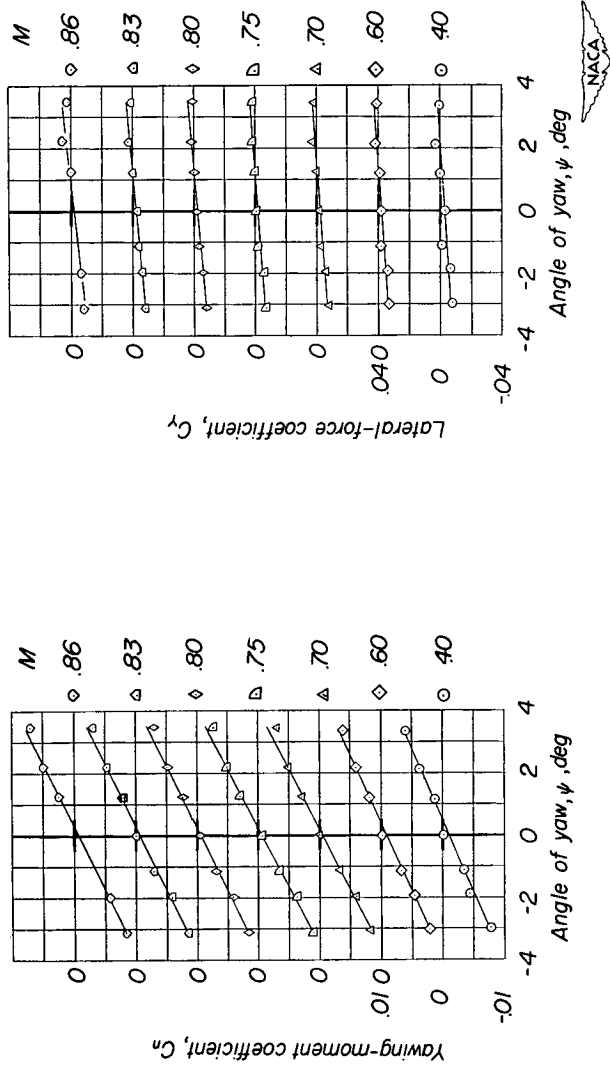


Figure 14.- Aerodynamic characteristics in yaw of the $\frac{1}{10}$ -scale model of the X-1 airplane.
 Horizontal and vertical tail off. $\alpha = 4^\circ$; $C_L \approx 0.60$.

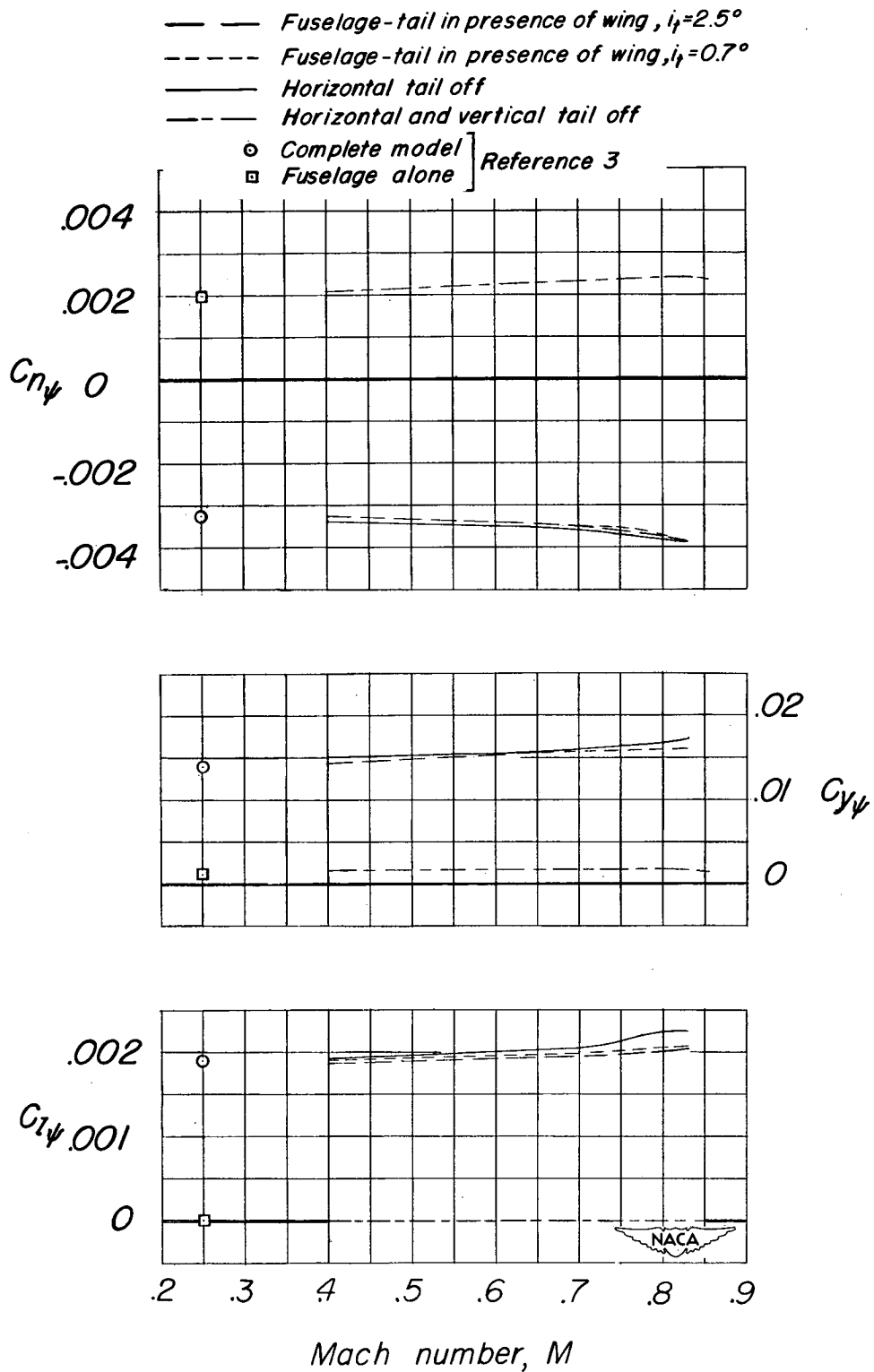


Figure 15.- Effect of Mach number on the lateral stability parameters of the $\frac{1}{10}$ -scale model of the X-1 airplane. $\alpha = 0^\circ$.

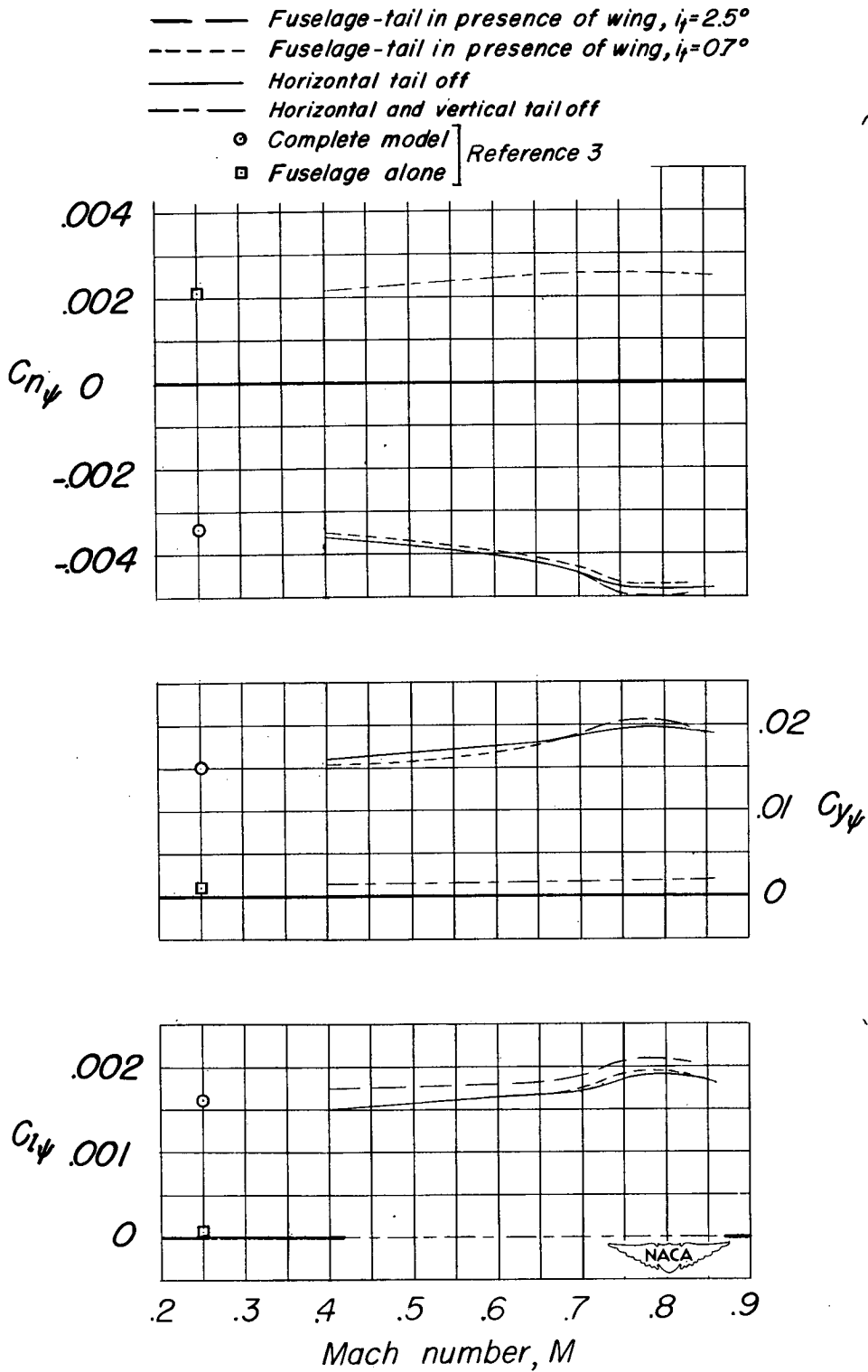


Figure 16.- Effect of Mach number on the lateral stability parameters of the $\frac{1}{10}$ -scale model of the X-1 airplane. $\alpha = 4^\circ$.

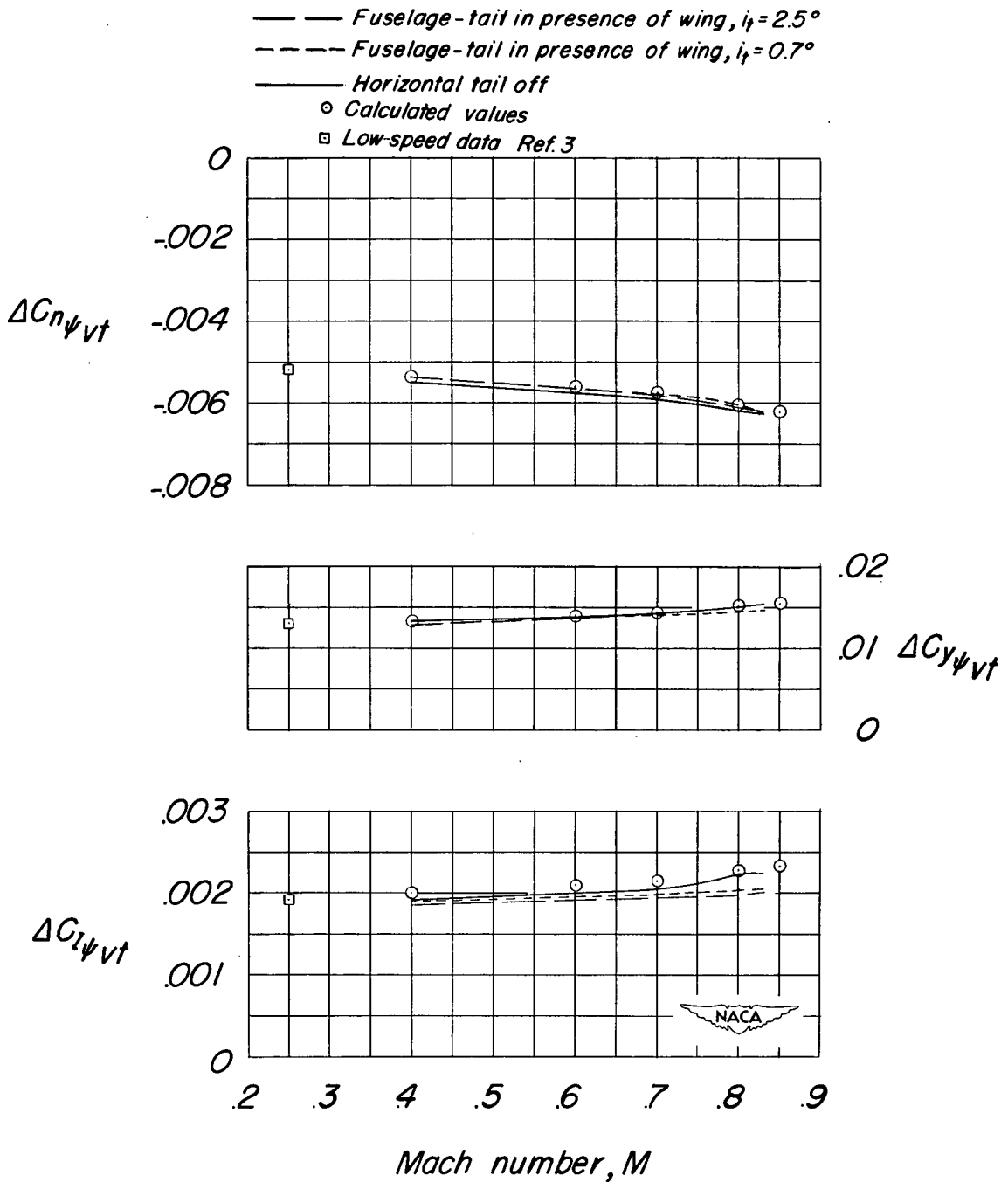


Figure 17.- Summary of experimental and calculated results on the effect of Mach number on the static lateral stability parameters of the X-1 airplane. $\alpha = 0^\circ$.